Since January 2020 Elsevier has created a COVID-19 resource centre with free information in English and Mandarin on the novel coronavirus COVID-19. The COVID-19 resource centre is hosted on Elsevier Connect, the company's public news and information website.

Neurochemistry International 138 (2020) 104779

Contents lists available at ScienceDirect

Neurochemistry International

journal homepage: www.elsevier.com/locate/neuint

Nicotinic acetylcholine receptors regulate clustering, fusion and acidification of the rat brain synaptic vesicles

Irene Trikash, Ludmila Kasatkina, Olena Lykhmus, Maryna Skok*

Palladin Institute of Biochemistry, NAS of Ukraine, Kyiv, Ukraine

ARTICLE INFO

Keywords:
Nicotinic acetylcholine receptor
Synaptic vesicles
Synaptic vesicle clustering
Membrane fusion
Levetiracetam

ABSTRACT

The brain nicotinic acetylcholine receptors (nAChRs) expressed in pre-synaptic nerve terminals regulate neurotransmitter release. However, there is no evidence for the expression of nAChRs in synaptic vesicles, which deliver neurotransmitter to synaptic cleft. The aim of this paper was to investigate the presence of nAChRs in synaptic vesicles purified from the rat brain and to study their possible involvement in vesicles life cycle. According to dynamic light scattering analysis, the antibody against extracellular domain (1–208) of α7 nAChR subunit inhibited synaptic vesicles clustering. Sandwich ELISA with nAChR subunit-specific antibodies demonstrated the presence of α4β2, α7 and α7β2nAChR subtypes in synaptic vesicles and showed that α7 and β2 nAChR subunits are co-localized with synaptic vesicle glycoprotein 2A (SV2A). Pre-incubation with either α7-selective agonist PNU282987 or nicotine did not affect synaptic vesicles clustering but delayed their Ca^{2+}-dependent fusion with the plasma membranes. In contrast, nicotine but not PNU282987 stimulated acidification of isolated synaptic vesicles, indicating that α4β2 but not α7-containing nAChRs are involved in regulation of proton influx and neurotransmitter refilling. Treatment of rats with levetiracetam, a specific modulator of SV2A, increased the content of α7 nAChRs in synaptic vesicles accompanied by increased clustering but decreased Ca^{2+}-dependent fusion. These data for the first time demonstrate the presence of nAChRs in synaptic vesicles and suggest an active involvement of cholinergic regulation in neurotransmitter release. Synaptic vesicles may be an additional target of nicotine inhaled upon smoking and of α7-specific drugs widely discussed as anti-inflammatory and pro-cognitive tools.

1. Introduction

Nicotinic acetylcholine receptors (nAChRs) are ligand-gated ion channels found in many types of both excitable and non-excitable cells. They mediate fast synaptic transmission in neuromuscular junctions and autonomic ganglia, whereas in the brain, they are localized mainly pre-synaptically to regulate neurotransmitter release (Dickinson et al., 2008; Gotti et al., 2009). In addition to plasma membrane, the nAChRs were discovered in the outer membrane of mitochondria to regulate the early events of mitochondria-driven-apoptosis (Gergalova et al., 2012; Skok et al., 2016). In contrast to muscular and ganglionic nAChRs, which mediate powerful ion currents, those expressed in the brain and mitochondria either mediate small local currents or function metabotropically by engaging the components of various intracellular signaling pathways (Papke, 2014; Skok et al., 2016).

Structurally, nAChRs are homo- or heteropentamers composed of 10 types of alpha (α1 to α10) and 4 types of beta (β1 to β4) subunits combined in several established combinations; muscular nAChRs also contain γ, δ and ε subunits (Fasoli and Gotti, 2015). The main nAChR subtypes found in the brain are α4β2 and α7 (Champtiaux and Changeux, 2002); α4β2 was shown to be critical for learning and memory (Picciotto et al., 2001), while α7-containing nAChRs control cell proliferation, survival (Resende and Adhikari, 2009) and inflammation (De Jonge and Ulloa, 2007) and are also important for cognition (Leiser et al., 2009; Lykhmus et al., 2020). The α7 nAChRs were initially discovered as homopentamers (Lindstrom, 1996); however, heteropentamers containing β2 subunits were further revealed in the brain (Moretti et al., 2014), autonomic ganglia (Cuevas et al., 2000) and mitochondria (Skok et al., 2016).

Synaptic vesicles (SVs) function in presynapse to store and deliver neurotransmitter to the synaptic cleft. During their life cycle, SVs pass through several stages of maturation like de novo biogenesis,

Abbreviations: AO, acridine orange; nAChR, nicotinic acetylcholine receptor; Lev, levetiracetam; PM, plasma membrane; R18, octadecyl rhodamine B; SVs, synaptic vesicles; SV2A, synaptic vesicle glycoprotein 2A

* Corresponding author. Palladin Institute of Biochemistry, 9, Leontovycha str., 01054, Kyiv, Ukraine.
E-mail address: skok@biochem.kiev.ua (M. Skok).

https://doi.org/10.1016/j.neuint.2020.104779
Received 13 April 2020; Received in revised form 20 May 2020; Accepted 25 May 2020
Available online 29 May 2020

acidification, accumulation of neurotransmitter and fusion with presynaptic plasma membrane (PM). Consequently, they contain plenty of specific proteins involved in SVs interaction with each other and with PM, neurotransmitter acquisition and release, etc. (Takamori et al., 2006). Although it is well established that the nAChRs expressed in presynaptic nerve terminals regulate the transmitter release (Dickinson et al., 2008), no direct evidence for the presence of nAChRs in SVs can be found in the literature. The early paper of Jacob et al. (1986), who studied the intracellular pool of nAChRs, demonstrated the nAChR-specific immunoreactivity in coated pits, coated vesicles, multivesicular bodies, and smooth-membraned vacuoles. Another paper shows that nicotine enhanced dopamine refilling and release from striatal synaptosomes, suggesting the involvement of two discrete nAChR subtypes (Turner, 2004). The aim of the present paper was to investigate the presence of nAChRs in SVs isolated from the rat brain and to study their possible involvement in vesicles life cycle.

2. Materials and methods

2.1. Materials

All reagents were purchased from Sigma-Aldrich (Saint Louis, USA), unless specially indicated. Acridine orange (AO), R18 (octadecyl rhodamine B chloride) were from Molecular Probe (Eugene, OR, USA.). Octaethyleneglycol-dodecyl ether (C12E8) was purchased from Calbiochem (USA). All chemicals used in the research were of analytical grade. Dilutions were made by deionized water.

Antibodies against α7(1–208) (Lykhmus et al., 2010), α3(181–192), α4(181–192), α7(179–190) (Skok et al., 1999), α9(11–23) (Koval et al., 2011), β2(190–200) or β4(190–200) (Koval et al., 2004) nAChR fragments were obtained, characterized and biotinylated previously in our lab. Neutravidin-peroxidase conjugate and SV2A-specific antibody (Invitrogen) were purchased from ALT Ukraine Ltd (representative of Thermo Fisher Scientific in Ukraine).

2.2. Animals

We used Wistar rats (6-month-old, males, 480–500 g) and C57Bl/6 mice, either wild-type or α7−/− (Orr-Urtreger et al., 1997) (2–3 months old females, 20–25 g). All animals were kept in the animal facility of Palladin Institute of Biochemistry at the 12 h light cycle. They were housed in a quiet, temperature-controlled room (22–23 °C) and were provided with water and dry food pellets ad libitum. Before removing the brain rats were anesthetized with isoflurane, while mice were sacrificed by cervical dislocation. All animal experiments complied with the ARRIVE guidelines and were carried out in accordance with the EU Directive 2010/63/EU for animal experiments. All procedures conformed to the guidelines of the Animal Care and Use Committee (IACUC) of Palladin Institute of Biochemistry, Kyiv. All efforts were made to minimize animal suffering and to reduce the number of animals used.

For Lev treatment protocol, rats were randomly distributed into two groups, 6 animals in each. Experimental group obtained Lev (60 mg/kg) per os once a day (Kasatkina et al., 2018). Control group received equivalent volume (100 μl) of vehicle (distilled water). Animals were sacrificed on day 15 of the experiment.

2.3. Isolation of synaptic vesicles, plasma membranes and mitochondria

Rat brains were weighed, cut into pieces, transferred to ice-cold 0.32 M sucrose, 10 mM Tris-HCL, pH 7.5 (9 ml/g of brain tissue) and gently homogenized using a glass homogenizer with a Teflon plunger (0.25 mm clearance). All manipulations were performed at 0°C. Synaptosomes were prepared by differential centrifugation of rat brain homogenate (De Lorenzo and Freedman, 1978). The resultant pellet (crude synaptosomes) was used to obtain PMs and SVs as described earlier (Trikash and Kolchinskaya, 2006).

The resultant pellet of synaptosomes was lysed with 1 mM EGTA, 10 mM Tris-HCl pH 8.1 at 4 °C for 60 min and centrifuged at 20000 g for 30 min. The pellet was used to separate the PMs, while the supernatant was centrifuged at 55000g, 60 min (pellet withdrawn) and again at 130000 g, at 4 °C, 60 min. The last centrifugation yielded SVs in the pellet and cytosolic synaptosomal proteins in the supernatant. The resulting SVs pellet was resuspended in 10 mMTris-HCl pH 7.5. The SVs fraction was characterized in detail by electron microscopy and laser correlation spectroscopy previously (Trikash et al., 2004).

For isolation of synaptic PMs, the pellet obtained after initial synaptosomes fractionation was resuspended in 0.32 M sucrose, 10 mMTris-HCl, pH 7.5 and layered on a discontinuous (0.8–1.1 M) sucrose gradient. Centrifugation was carried out in the bucket-rotor at 50000 g for 120 min. Membrane fraction was collected at the interface between 0.8 M and 1.1 M sucrose and 4 vol of 10 mMTris-HCl, pH 7.5 was added. This suspension was centrifuged at 130000 g for 10 min. Finally, the pellet was resuspended in 0.32 M sucrose, 10 mM Tris-HCl, pH 7.5. Purified PMs were used for the membrane fusion and ELISA studies.

Mitochondria were isolated from the brain homogenate of either rats or mice by differential centrifugation according to standard published procedures (Sottocasa et al., 1967; Gergalova et al., 2012). Their purity was characterized by ELISA using the antibodies against voltage-dependent anion channel (VDAC, mitochondria marker) as described (Uspenska et al., 2017). Mitochondria of the wild-type and α7−/− mice were isolated in Kyiv, while those of β2−/− mice were obtained in the Institut Pasteur in Paris in the course of previous collaborative studies.

To prepare detergent lysates, the pellets of PMs, SVs or mitochondria were frozen at −20 °C, thawed and treated with lysing buffer (0.01 M Tris-HCl, pH 8.0; 0.14 NaCl; 0.025% NaN_3; 1% Tween-20 and protease inhibitors cocktail) for 2 h on ice upon intensive stirring. The resulting lysates were pelleted by centrifugation (20 min at 20,000g). The protein concentration was established with the BCA Protein Assay kit (Thermo Scientific, Rockford, USA).

2.4. Sandwich assays

To determine the level of various nAChR subunits within the brain PMs, SVs or mitochondria preparations, the immunoplates (Nunc, Maxisorp) were coated with rabbit α7(1–208)-specific antibody (20 μg/ml), blocked with 1% BSA, and the detergent lysates of the membranes, SVs or mitochondria were applied into the wells (1 μg of protein per 0.05 ml per well) for 2h at 37 °C. The plates were washed with water and the second biotinylated α3(181–192)-, α4(181–192)-, α7(179–190)-, α9(11–23)-, β2(190–200)- or β4(190–200)-specific antibody was applied for additional 2 h. All antibodies have been preliminary titrated in corresponding antigenic peptides and the doses (dilutions) have been selected according to titration curves: 1:200 for α3-specific, 1:80 for α4-specific, 1:300 for α7-specific, 1:250 for α9-specific, 1:250 for α10-specific, 1:500 for β2-specific and 1:200 for β4-specific, assuming that the initial concentration of all antibodies was 2 mg/ml.

To evaluate the presence of α4β2 and α7β2 combinations, the plates were coated with α4(181–192)- or α7(179–190)-specific antibodies (20 μg/ml), mitochondria and SVs preparations were applied as described above and the bound β2 subunits were revealed with β2(190–200)-specific antibody (1:500).

To test the presence of nAChR complexes with SV2A protein, the plates were coated with SV2A-specific antibody (10 μg/ml) and the bound nAChRs from SVs preparation were revealed with biotinylated α3(181–192)-, α4(181–192)-, α7(179–190)-, α9(11–23)-, β2(190–200)- or β4(190–200)-specific antibodies as described above.

The bound biotinylated antibodies were revealed with Neutravidin-peroxidase conjugate and *o*-phenylendiamine-containing substrate

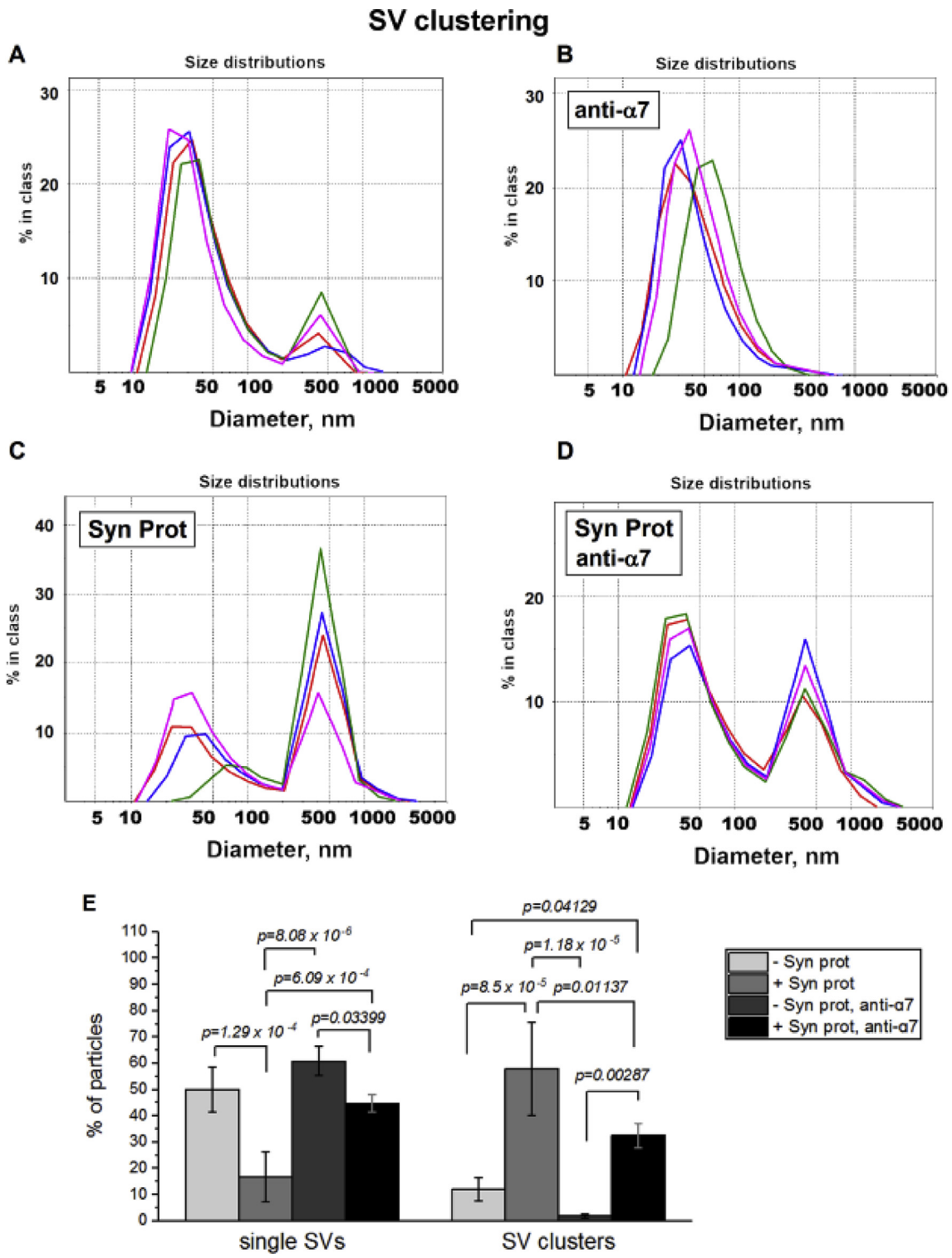

Fig. 1. Initial histograms (**A-D**) and a summarizing graph (**E**) of single SVs (30–60 nm) and SV clusters (250–900 nm) estimated by dynamic light scattering in buffer (**A-B**) or in the presence of cytosolic synaptic proteins (SynProt, **C-D**) in the absence (**A, C**) or presence (**B, D**) of α7(1–208)-specific antibody (anti-α7). Each curve in **A-D** corresponds to separate measurement; each column in **E** corresponds to M ± SD, n = 4. According to post-hoc Tukey's test after significant overall two-way ANOVA, for single SVs, cytosolic proteins: $F = 47.93479$; $p = 1.59717 \times 10^{-5}$; anti-α7: $F = 29.87625$; $p = 1.43927 \times 10^{-4}$; for SV clusters, cytosolic proteins: $F = 66.27568$; $p = 3.14272 \times 10^{-6}$; anti-α7: $F = 14.33388$; $p = 0.0026$.

solution. The optical density of ELISA plates was read at 490 nm using Stat-Fax 2000 ELISA Reader (Awareness Technologies, USA).

2.5. Dynamic light scattering (DLS)

The hydrodynamic diameter of the particles in SVs suspension was measured using Malvern 4700 Zetasizer-3 spectrometer (Malvern Instruments, Worcestershire, U.K.) equipped with helium-neon laser

"LG-111" (25 mW; wavelength 632.8 nm). Vesicle suspension (50 μl, 50 μg) was injected into cuvette containing 950 μl of either the lysis buffer (1 mM EGTA and 10 mM Tris-HCl, pH 8.1) or solution of synaptosomal cytosolic proteins (1 mg/ml). DLS measurements were carried out at a room temperature (22–24 °C). The scattering was detected at the angle of 90°. Data were analyzed by Contin algorithm (Malvern Instruments), which calculates the Z-average size and polydispersity. The transforms of the intensity distribution to volume distributions were calculated using Malvern Instruments software.

2.6. R18 assay for monitoring the membrane fusion

The R18 assay is based on the changes of fluorescence intensity upon fusion of R18-labeled SVs and unlabeled PMs. SVs were labeled with R18 (20 μM) as described earlier (Kasatkina et al., 2018) and preincubated with vehicle, 75 nM nicotine or 30 nM PNU282987 for 10 min at 37 °C. These SVs (3 μl) were mixed with unlabeled PMs (1:9, based on protein concentration) in the medium of cytosolic synaptic proteins and supplemented with 10^{-5} M Ca^{2+} (start point, Trikash et al., 2010). R18 fluorescence was recorded during 4 min thereafter by spectrofluorimeter Hitachi 650-10S (Japan) at excitation and emission wavelength of 560 and 580 nm respectively with the 5 nm slit width and 530 nm cut-off filter in the emission beam. At the end of each experiment octaethyleneglycol-dodecyl ether (final concentration of 0.1%) was added to the reaction mixture to yield maximal fluorescence dequenching.

Fusion was registered as an increase of R18 fluorescence after lipid bilayer intermixing. The rate of fusion was proportional to the percentage of fluorescence dequenching (%FD):

$$\% \text{ FD} = 100(I - I_o) / (I_d - I_o)$$

Where I_o is the initial fluorescence signal of R18-labeled SVs, I is the signal measured during the experiment and I_d is the maximum value of the dequenched fluorophore signal after addition of octaethyleneglycol-dodecyl ether.

2.7. Registration of SVs acidification

The changes in the SVs acidic state were registered with pH-sensitive fluorescent dye acridine orange (AO), which is accumulated in intracellular compartments proportionally to their pH values. Acidification of SVs results in decrease of AO green fluorescence.

Isolated SVs at a final protein concentration of 0.3 mg/ml were preincubated at 37 °C for 10 min and fluorescence measurements were performed with spectrofluorimeter Hitachi 650-10S (Japan) at the excitation and emission wavelengths of 490 and 530 nm, correspondingly, with 2 nm slit width. Nicotine or PNU282987 were added at the plateau level of dye fluorescence intensity. Traces were normalized to the similar recordings in the absence of SVs by the equation:

$$F = F_t / F_0$$

where F_0 is the fluorescence intensity of AO in solution, and F_t is the fluorescence intensity of AO in the presence of isolated synaptic vesicles.

2.8. Statistical analysis

ELISA experiments have been performed in triplicates and mean values were used for statistical analysis assessed using one-way ANOVA test. The fluorescent and DLS data were performed in quadruplicates and analyzed by one-way or two-way ANOVA (as indicated). The data are presented as Mean ± SD, the *p* and F values are shown either in the figures or in the figure legends.

3. Results

Dynamic light scattering of SVs preparations demonstrated the presence of two peaks corresponding to particles of about 40 and 500 nm diameters both in the buffer and in the presence of cytosolic synaptic proteins (Fig. 1A–D). The size of the smaller peak corresponded to reported SVs size (Mundigl and De Camilli, 1994, https://www.ncbi.nlm.nih.gov/pubmed/?term=De%20Camilli%20P%5BAuthor%5D&cauthor=true&cauthor_uid=7986534). Cytosolic proteins are known to promote the SVs clustering by bringing them into close proximity, where they become stably bound or docked (Rottman, 1994; Trikash and Kolchinskaya, 2006; Trikash et al., 2008; Kasatkina et al., 2020). When SVs were tested in buffer, the peak of single SVs prevailed (Fig. 1A) and the peak of larger size particles (SV clusters) obviously increased in the presence of cytosolic proteins (Fig. 1C). Addition of α7(1–208)-specific antibody to the incubation medium resulted in complete disappearance of SVs clusters found in buffer (Fig. 1B) and in obvious decrease of clusters number in favor of single SVs when cytosolic proteins were present in the incubation medium (Fig. 1D, summarized in Fig. 1E). These data indicated that α7(1–208)-specific antibody prevents (in buffer) or inhibits (in protein medium) SVs clusters formation suggesting the nAChRs involvement.

The antibody elicited against the large extracellular domain (1–208) of α7 subunit potentially recognizes almost all nAChR subunits due to substantial homology of their extracellular portions. To determine the subunit composition of nAChRs within the SVs preparation we performed Sandwich ELISA, where the brain SVs, mitochondria or plasma membrane preparations were captured with α7(1–208)-specific antibody and were revealed with nAChR subunit-specific antibodies. Such an approach was successfully used by us previously to determine the nAChR subunits content in the brain (Lykhmus et al., 2017), B lymphocytes (Koval et al., 2011) and mitochondria preparations (Lykhmus et al., 2014). As shown in Fig. 2A, synaptic vesicles demonstrated positive signals for α3, α4, α7, α9, β2 and β4 nAChR subunits. Provided similar protein quantity was applied, the SVs nAChR composition was closer to the brain mitochondria than to brain PMs, the main subunits being α4, α7 and β2.

The α4 subunits form an established combination with β2 subunits in the brain, while α7 subunits can form either homopentamers or heteromers with β2 subunits (Lindstrom, 1996; Khiroug et al., 2002). To study which combinations are found in SVs, we performed another Sandwich ELISA, where the preparation was captured with α4-or α7-specific antibody and revealed with β2-specific antibody. As shown in Fig. 2B, a strong signal for α4β2 combination was found in both SVs and mitochondria. The signal for α7β2 combination was much weaker compared to α4β2 and was significantly higher in SVs compared to mitochondria. Since the total signals for α4, α7 and β2 subunits in SVs were quite similar and high (Fig. 2A), the data obtained with α4/β2 and α7/β2 antibody pairs suggested that only a part of α7 subunits found in SVs form heteromeric α7β2 nAChRs. The specificity of antibodies towards α7 or β2 nAChR subunits was confirmed in the assay using mitochondria of the wild-type, α7−/− or β2−/− mice. As shown in Fig. 2C, mitochondria of the wild-type mice gave positive signals in both α7 and α7β2 assays, α7−/− mitochondria were negative in both assays, while β2−/− mitochondria were positive for α7 but not α7β2.

We further performed Sandwich ELISA where the preparation was captured by the antibody against a synaptic vesicle protein SV2A (Feany, 1992) and revealed with nAChR subunit-specific antibodies. Positive signals were found mainly for α7-and β2-specific antibodies suggesting the co-localization of SV2A with α7 and β2 nAChR subunits on SVs (Fig. 2D).

Based on the results of Sandwich ELISA experiments, further studies were performed using an α7-selective agonist PNU282987 (30 nM) and nicotine (75 nM), mostly specific for α4β2 nAChRs (Wonnacott, 2014). We applied them in either dynamic light scattering analysis or in R18 assay, which measure SVs clustering or fusion, respectively. It was

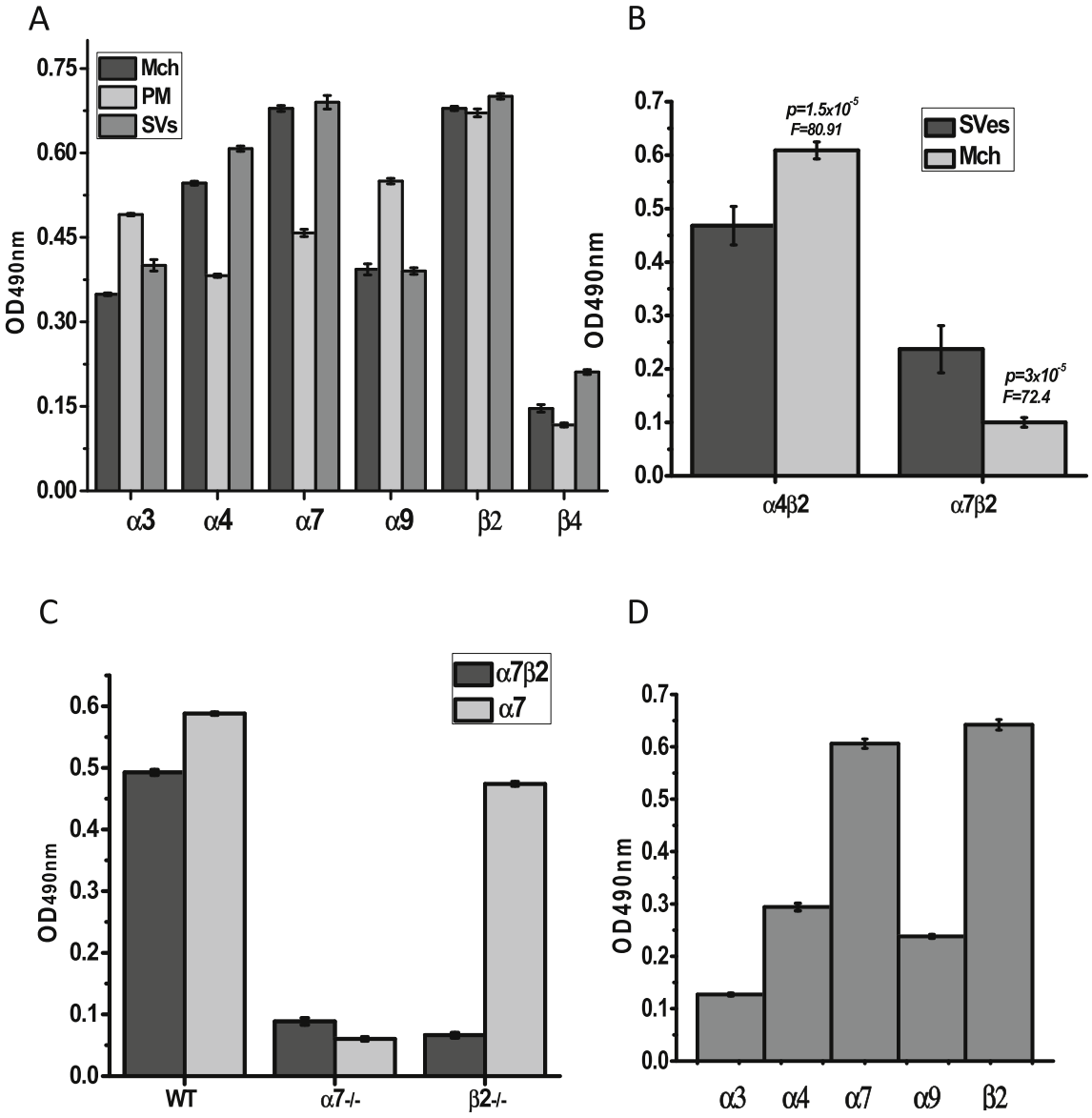

Fig. 2. Sandwich ELISA of the brain mitochondria (Mch), plasma membranes (PM) and synaptic vesicles (SVs) preparations. **A** – the content of nAChR subunits in SVs compared to Mch and PM; **B**– the level of α4β2 and α7β2 combinations in Mch and SVs; **C** – the content of α7 and α7β2 nAChRs in mitochondria of the wild-type (WT), α7−/− or β2−/− mice; **D** - combinations of nAChR subunits with SV2A protein in synaptic vesicles. Each column corresponds to M ± SD of triplicate measurements; the *p* and F values measured by one-way ANOVA are shown in the figure.

found that SVs pre-incubation with either PNU282987 or nicotine did not affect SV clustering (Fig. 3A) but delayed their Ca^{2+}-dependent fusion with the PM by 47.5% and 58.8%, respectively (Fig. 3B). In contrast, 1 μM nicotine but not 30 nM PNU282987 stimulated acidification of isolated SVs, as measured by the fluorescence of pH-sensitive dye acridine orange (Fig. 4) indicating that α4β2 but not α7-containing nAChRs are involved in regulation of proton influx in SVs.

SV2A was identified as a specific binding site for levetiracetam (Lev), a second generation antiepileptic drug (Cortes-Altamirano et al., 2016). Taking into account the established co-localization of SV2A with α7 and β2 nAChR subunits (Fig. 2D), we studied the effect of Lev treatment on SVs properties and nAChR composition. As shown in Fig. 5, treatment of rats with Lev for two weeks increased their SVs clustering (Fig. 5A) but decreased Ca^{2+}-dependent fusion with the PM (Fig. 5B) compared to SVs of non-treated rats. Sandwich ELISA demonstrated that Lev treatment decreased α4 and β2 nAChR subunits in both synaptic PMs and SVs, while α7 subunit was found decreased in PMs and increased in SVs (Fig. 6A and B). Therefore, Lev treatment resulted in redistribution of homomeric α7 nAChRs in favor of SVs. In addition, significant increase was found for α9 subunit in SVs, whereas β4 subunits were up-regulated in the PMs.

4. Discussion

Functional nAChRs were traditionally attributed exclusively to cell PM; the intracellular pool was considered as non-mature nAChRs on the way of biosynthesis. The discovery of mitochondrial nAChRs showed for the first time that these receptors can function in intracellular environment (Gergalova et al., 2012). The data presented here reveal one more intracellular compartment where nAChRs seem to play a significant role: they demonstrate the presence of nAChRs in SVs and their functional role in sequential steps of SV release.

The nAChRs can penetrate into SVs either from the endosomes in the course of SVs biogenesis, or from the PM in the course of SVs recycling (Bonanomi et al., 2006). The Lev treatment affected the PM and vesicular nAChRs in different ways that is in favor of independent ways

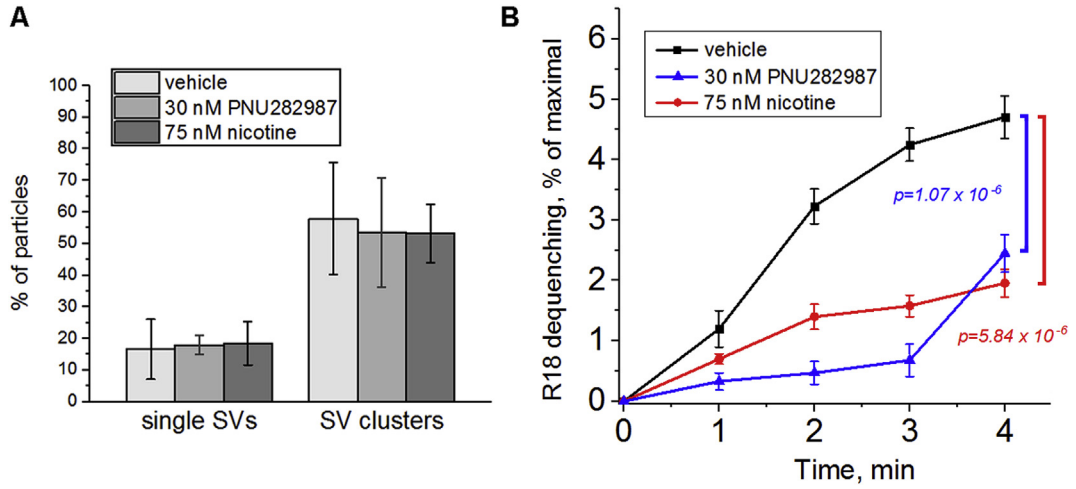

Fig. 3. SV clusters formation estimated by dynamic light scattering (**A**) and Ca^{2+}-triggered fusion with PMs analyzed by R18 fusion assay (**B**) after pre-incubation with 30 nM PNU282987, 75 nM nicotine or vehicle. Each column (A) or point on the curve (B) corresponds to M ± SD, n = 4; post-hoc Tukey's test after significant overall one-way ANOVA ($F = 94.6727$; $p = 9.03008 \times 10^{-7}$).

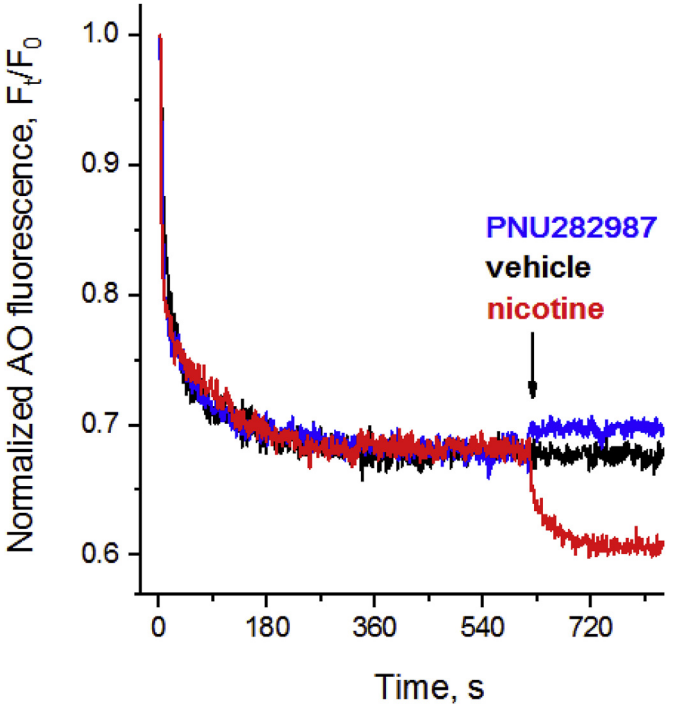

Fig. 4. The acute effect of nicotine (1 μM) and PNU282987 (30 nM) on vesicular ΔpH measured with pH-sensitive dye acridine orange (AO). Fluorescence traces were normalized to the AO fluorescence decay in the absence of SVs. Shown are typical traces of four independent measurements.

of their trafficking. However, an obvious re-distribution of α7 nAChRs between SVs and PMs may be a sign of selective re-uptake of this nAChR subtype from the membrane in the course of SVs recycling. The antibody specific to the nAChR extracellular domain (1–208) influenced SVs clusters formation suggesting that the nAChRs are located on the vesicle surface facing an extravesicular environment. The immediate effect of nicotine on SVs acidification and fast effects of nicotine and PNU282987 on SVs fusion are also in favor of an outward localization of nAChRs on SVs surface. The mechanisms of the nAChR trafficking to and incorporation into SVs need further examination.

The similarity of SVs nAChR content to mitochondrial and not to PM one might be a sign of independent trafficking of newly synthesized nAChRs to either the PM or intracellular compartments. However, the nAChR subunits content was normalized to similar quantity of protein loaded in ELISA. Both SVs and mitochondria preparations contain internal proteins, in addition to membrane ones, therefore, the relation of nAChRs to general protein content is lower compared to purified plasma membranes. Also, we cannot exclude that the density of nAChRs in mitochondria and SVs is lower compared to plasma membranes, which contain highly concentrated nAChRs in synaptic areas.

The presence of α4β2 and α7(β2) nAChRs in SVs and their changes upon Lev administration suggested the importance of cholinergic regulation for SVs functions. Here we studied three processes related to SVs life cycle and functioning: acidification (proton pumps activity as the driving force to refill vesicles with the neurotransmitter), clusters formation and Ca^{2+}-dependent fusion with the PM resulting in exocytosis and neurotransmitter release.

The cell-free system, which simulates SVs interaction with each other and/or with the plasma membrane during the exocytotic process in presynapse, allowed us to investigate which steps of this process are affected by Lev treatment or nAChR agonists. The increase of vesicular ΔpH upon nicotine application suggests that the storage capacity of SVs can be positively regulated by cytosolic nicotine through activation of vesicular nAChRs. At least this is true for the vesicular transport of monoamines, acetylcholine, GABA and glycine where ΔpH is a main or prevailing driving force for accumulation.

Up-regulation of α7 (and α9) nAChRs in SVs of Lev-treated rats was accompanied by increased SVs clustering but decreased fusion with the PM. This is in accord with already reported Lev effect on α7 nAChR signaling (Tsudaka et al., 2015). Accordingly, anti-α7(1–208) antibody prevented SVs clusters formation, while PNU282987 and nicotine delayed SVs fusion. Taken together, this data suggest that the nAChRs expressed in SVs favor their clustering but prevent fusion.

Nicotine and PNU282987 prevented SVs fusion with the plasma membranes but did not influence SVs clustering. Therefore, the nAChR ion channel activity negatively regulates fusion but is not critical for intra-vesicles interaction. However, SVs clustering was impaired by α7(1–208)-specific antibody and the changes in SVs nAChR content in Lev-treated rats were accompanied by increased SVs clustering suggesting that the nAChRs may be involved in ion-independent manner, possibly, due to their connection to SV2A.

The discovery of functional nAChRs in SVs naturally puts a question about their physiological significance and the ligands, which affect them inside the cell. The α7-containing nAChRs can be activated by choline readily available intracellularly (Alkondon and Albuquerque, 2006). It was recently shown that α9-containing nAChRs can be activated by phosphocholine and phosphocholine-modified

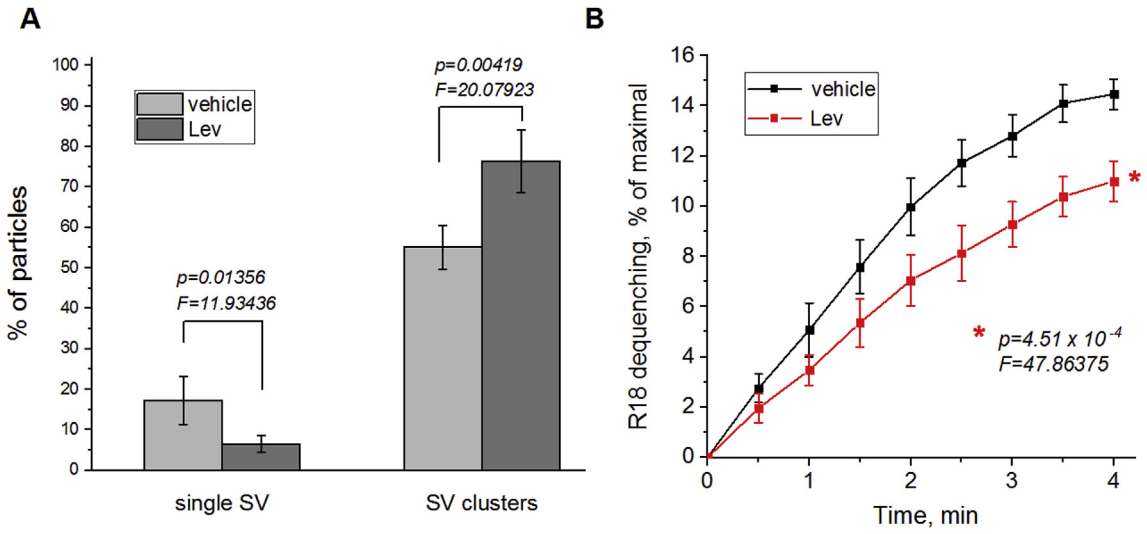

Fig. 5. Clusters formation estimated by dynamic light scattering (**A**) and Ca^{2+}-triggered fusion with PMs analyzed by R18 fusion assay (**B**) of SVs obtained from either vehicle- or levetiracetam-treated rats. Each column (**A**) or point on the curve (**B**) corresponds to M ± SD, n = 4; the *p* and F values measured by one-way ANOVA are shown in the figure.

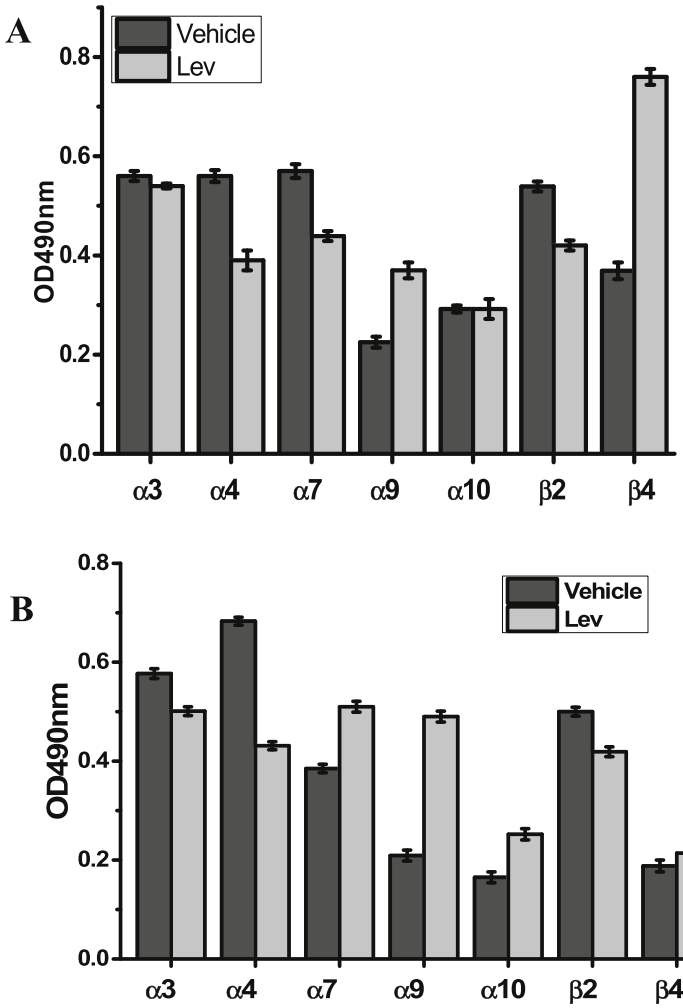

	p	F
α3	0.002	132.6
α4	$2x10^{-6}$	1540.5
α7	$1.2x10^{-6}$	235.1
α9	$1.8x10^{-6}$	2035.2
α10	0.97	184.02
β2	$7.2x10^{-7}$	112.1
β4	$3.3x10^{-7}$	11.4

	p	F
α3	$5.2x10^{-4}$	26.3
α4	$2.5x10^{-6}$	314.3
α7	$1.1x10^{-4}$	378.1
α9	$5.8x10^{-6}$	328.5
α10	$6.1x10^{-5}$	118
β2	$4.5x10^{-4}$	958
β4	0.015	1280

Fig. 6. Sandwich ELISA of the PMs (**A**) or SVs (**B**) obtained from the brains of vehicle-treated (Ctrl) or Lev-treated rats (n = 4). Each column corresponds to M ± SD of triplicate measurements; the *p* and F values measured by one-way ANOVA are shown in the figure.

macromolecules (Richter et al., 2016). Our unpublished data allow suggesting that phosphocholine also affects α7 nAChRs. Recently published evidence demonstrates that long-chain unsaturated acylcholines can be viewed as endogenous modulators of α7 nAChRs (Akimov et al., 2020) These choline derivatives are natural components of membrane lipids, which, similarly to α7 nAChRs agonists, can affect SVs fusion with the PM and the process of neurotransmitter release.

In contrast to fusion, which was affected similarly by nicotine and PNU282987 activating both α4β2 and α7(β2) nAChRs, SVs acidification was affected by nicotine only suggesting that α7 nAChRs are not involved in regulating the proton flux (i.e. V-type H^+-ATPase and cation/H^+ exchangers). The α4β2 nAChRs cannot be activated by choline. However, SVs loading with acetylcholine assumes their contact with this neurotransmitter. The data presented here suggest that activating α4β2 nAChRs by acetylcholine can stimulate its penetration into SVs. A question remains whether α4β2 nAChRs are expressed in SVs of cholinergic neurons only. If so, such neurons may have a specific way of regulation of neurotransmitter release, not available in other cells. This should be examined in future experiments.

It is well established that the brain nAChRs are located mainly presynaptically to regulate the release of several neurotransmitters (Dickinson et al., 2008). Application of nicotine to striatal nerve terminals (synaptosomes) promoted a sustained efflux of dopamine by affecting two different nAChR subtypes (Turner, 2004). Our data for the first time show the presence of nAChRs in synaptic vesicles (previously considered as passive transport vehicles) and suggest a new way of cholinergic regulation of neurotransmitter release. According to this suggestion, synaptic vesicles may be an additional target of nicotine inhaled upon smoking and of α7-specific drugs widely discussed as anti-inflammatory and pro-cognitive tools. A potential connection of α7 nAChRs and SV2A and a significant increase of α9 and α7 nAChRs in SVs of Lev-treated rats suggest an important role of nAChRs in regulating pro-epileptic activity and an additional mechanism of Lev anti-epileptic effect. SV2A, a specific target of Lev, is prevailing SV2 isoform in most GABAergic neurons and in granule cells of dentate gyrus (Bajjalieh et al., 1994), which controls hippocampal excitability. SV2 directly interacts and co-traffics with calcium sensor protein synaptotagmin and plays a major role in regulating the amount of this protein in SVs (Yao et al., 2010). In light of recent publications about the involvement of nAChRs in COVID-19 pathogenesis (Changeux et al., 2020), the finding of nAChRs in SVs can explain the neurological effects of SARS-Cov2, in particular, seizures provoked by SARS-CoV-2 infection in patients with epilepsy (Vollono et al., 2020).

Funding

This work was funded by the budget program of National Academy of Sciences of Ukraine, “Support for the development of priority areas of scientific research”, code 6541230, project No. 28/2018–2019, and the joint Ukraine-Austria R&D project No. UA 09/2017 of the Austrian Agency for International Cooperation in Education and Research (OeAD) and the Ministry of Education and Science of Ukraine.

Author statement

Irene Trikash: Conceptualization, Methodology, Investigation, Writing –Reviewing and Editing. Ludmyla Kasatkina: Investigation, Visualization, Data curation, Writing- Reviewing and Editing. **Olena Lykhmus**: Investigation, Visualization, Data curation, Writing-Reviewing and Editing. **Maryna Skok**: Conceptualization, Writing-Original draft preparation, Writing- Reviewing and Editing.

Acknowledgement

We are grateful to Dr Yu. Chunikhin for the help in dynamic light scattering studies.

References

Akimov, M.G., Kudryavtsev, D.S., Kryukova, E.V., Fomina-Ageeva, E.V., Zakharov, S.S., Gretskaya, N.M., Zinchenko, G.N., Serkov, I.V., Makhaeva, G.F., Boltneva, N.P., Kovaleva, N.V., Serebryakova, O.G., Lushchekina, S.V., Palikov, V.A., Palikova, Y., Dyachenko, I.A., Kasheverov, I.E., Tsetlin, V.I., Bezuglov, V.V., 2020. Arachidonoylcholine and other unsaturated long-chain acylcholines are endogenous modulators of the acetylcholine signaling system. Biomolecules (2), 283. https://doi.org/10.3390/biom10020283.

Alkondon, M., Albuquerque, E.X., 2006. Subtype-specific inhibition of nicotinic acetylcholine receptors by choline: a regulatory pathway. J. Pharmacol. Exp. Therapeut. 318, 268–275.

Bajjalieh, S.M., Franz, G., Weimann, J.M., McConnell, S.K., Scheller, R.H., 1994. Differential expression of synaptic vesicle protein 2 (SV2) isoforms. J. Neurosci. 14, 5223–5235.

Bonanomi, D., Benfenati, F., Valtorta, F., 2006. Protein sorting in the synaptic vesicle life cycle. Prog. Neurobiol. 80, 177–217.

Champtiaux, N., Changeux, J.P., 2002. Knock-out and knock-in mice to investigate the role of nicotinic receptors in the central nervous system. Curr. Drug Targets - CNS Neurol. Disord. 1 (4), 319–330.

Changeux, J., Amoura, Z., Rey, F., Miyara, M., 2020. A nicotinic hypothesis for Covid-19 with preventive and therapeutic implications. Preprint V2. Qeios. https://doi.org/10.32388/FXGQSB.2.

Cortes-Altamirano, J.L., Olmos-Hernández, A., Bonilla-Jaime, H., Bandala, C., González-Maciel, A., Alfaro-Rodríguez, A., 2016. Levetiracetam as an antiepileptic, neuroprotective, and hyperalgesic drug. Neurol. India 64 (6), 1266–1275. https://doi.org/10.4103/0028-3886.193801.

Cuevas, J., Roth, A.L., Berg, D.K., 2000. Two distinct classes of functional α7-containing nicotinic receptor on rat superior cervical ganglion neurons. J. Physiol. 525 (Pt 3), 735–746.

De Jonge, W.J., Ulloa, L., 2007. The alpha7 nicotinic acetylcholine receptor as a pharmacological target for inflammation. Br. J. Pharmacol. 151, 915–929.

DeLorenzo, R.J., Freedman, S.D., 1978. Calcium dependent neurotransmitter release and protein phosphorylation in synaptic vesicles. Biochem. Biophys. Res. Commun. 80 (1), 183–192. https://doi.org/10.1016/0006-291x(78)91121-x.

Dickinson, J.A., Kew, J.N., Wonnacott, S., 2008. Presynaptic alpha 7- and beta 2-containing nicotinic acetylcholine receptors modulate excitatory amino acid release from rat prefrontal cortex nerve terminals via distinct cellular mechanisms. Mol. Pharmacol. 74 (2), 348–359.

Fasoli, F., Gotti, C., 2015. Structure of neuronal nicotinic receptors. Curr.Top.Behav.Neurosci. 23, 1–17.

Feany, M.B., 1992. The synaptic vesicle protein SV2 is a novel type of transmembrane transporter. Cell 70 (5), 861–867.

Gergalova, G.L., Lykhmus, O.Yu, Kalashnyk, O.M., Koval, L.M., Chernyshov, V.O., Kryukova, E.A., Tsetlin, V.I., Komisarenko, S.V., Skok, M.V., 2012. Mitochondria express α7 nicotinic acetylcholine receptors to regulate Ca^{2+} accumulation and cytochrome *c* release: study on isolated mitochondria. PLoS One7(2), e31361.

Gotti, C., Clementi, F., Fornari, A., Gaimarri, A., Guiducci, S., Manfredi, I., Moretti, M., Pedrazzi, P., Pucci, L., Zoli, M., 2009. Structural and functional diversity of native brain neuronal nicotinic receptors. Biochem. Pharmacol. 78 (7), 703–711doi. https://doi.org/10.1016/j.bcp.2009.05.024.

Jacob, M.H., Lindstrom, J.M., Berg, D.K., 1986. Surface and intracellular distribution of a putative neuronal nicotinic acetylcholine receptor. J. Cell Biol. 103 (1), 205–214.

Kasatkina, L.A., Tarasenko, A.S., Krupko, O.O., Kuchmerovska, T.M., Lisakovska, O.O., Trikash, I.O., 2020. Vitamin D deficiency induces the excitation/inhibition brain imbalance and the proinflammatory shift. Int. J. Biochem. Cell Biol. 119, 105665. https://doi.org/10.1016/j.biocel.2019.105665.

Kasatkina, L.A., Gumenyuk, V.P., Sturm, E.M., Heinemann, A., Bernas, T., Trikash, I.O., 2018. Modulation of neurosecretion and approaches for its multistep analysis. Biochim. Biophys. Acta Gen. Subj. 1862 (12), 2701–2713.

Khiroug, S.S., Harkness, P.C., Lamb, P.W., Sudweeks, S.N., Khiroug, L., Millar, N.S., Yakel, J.L., 2002. Rat nicotinic ACh receptor alpha7 and beta2 subunits co-assemble to form functional heteromeric nicotinic receptor channels. J. Physiol. 540 (Pt 2), 425–434. https://doi.org/10.1113/jphysiol.2001.013847.

Koval, L., Lykhmus, O., Zhmak, M., Khruschov, A., Tsetlin, V., Magrini, E., Viola, A., Chernyavsky, A., Qian, J., Grando, S., Komisarenko, S., Skok, M., 2011. Differential involvement of α4β2, α7 and α9α10 nicotinic acetylcholine receptors in B lymphocyte activation in vitro. Int. J. Biochem. Cell Biol. 43, 516–524.

Koval, O.M., Voitenko, L.P., Skok, M.V., Lykhmus, E.Y., Tsetlin, V.I., Zhmak, M.N., Skok, V.I., 2004. The β-subunit composition of nicotinic acetylcholine receptors in the neurons of the Guinea pig inferior mesenteric ganglion. Neurosci. Lett. 365 (2), 143–146.

Leiser, S.C., Bowlby, M.R., Comery, T.A., Dunlop, J., 2009. A cog in cognition: how the alpha7 nicotinic acetylcholine receptor is geared towards improving cognitive deficits. Pharmacol. Ther. 122, 302–311.

Lindstrom, J., 1996. Neuronal nicotinic acetylcholine receptors. In: In: Narahashi, T. (Ed.), Ion Channels, vol. 4. Plenum Press, New York, pp. 377–449.

Lykhmus, O., Gergalova, G., Koval, L., Zhmak, M., Komisarenko, S., Skok, M., 2014. Mitochondria express several nicotinic acetylcholine receptor subtypes to control various pathways of apoptosis induction. Int. J. Biochem. Cell Biol. 53, 246–252.

Lykhmus, O., Voytenko, L., Lips, K.S., Bergen, I., Krasteva-Christ, G., Vetter, D.E., Kummer, W., Skok, M., 2017. Nicotinic acetylcholine receptor α9 and α10 subunits are expressed in the brain of mice. Front. Cell. Neurosci. 11, 282.

Lykhmus, O.Yu, Kalashnyk, O.M., Uspenska, K.R., Skok, M.V., 2020. Positive allosteric modulation of alpha7 nicotinic acetylcholine receptors transiently improves memory

but aggravates inflammation in LPS-treated mice. Front. Ageing Neurosci. 11https://doi.org/10.3389/fnagi.2019.00359. article 359.
Lykhmus, O., Koval, L., Pavlovych, S., Zouridakis, M., Zisimopoulou, P., Tzartos, S., Tsetlin, V., Volpina, O., Cloëz-Tayarani, I., Komisarenko, S., SkokM, 2010. Functional effects of antibodies against non-neuronal nicotinic acetylcholine receptors. Immunol. Lett. 128, 68–73.
Moretti, M., Zoli, M., George, A.A., Lukas, R.J., Pistillo, F., Maskos, U., Whiteaker, P., Gotti, C., 2014. The novel α7β2-nicotinic acetylcholine receptor subtype is expressed in mouse and human basal forebrain: biochemical and pharmacological characterization. Mol. Pharmacol. 86 (3), 306–317. https://doi.org/10.1124/mol.114.093377.
Mundigl, O., De Camilli, P., 1994. Formation of synaptic vesicles. Curr. Opin. Cell Biol. 6 (4), 561–567. https://doi.org/10.1016/0955-0674(94)90077-9.
Orr-Urtreger, A., Goldner, F.M., Saeki, M., Lorenzob, I., Goldberg, L., De Biasi, M., et al., 1997. Mice deficient in the α7 neuronal nicotinic acetylcholine receptor lack α-bungarotoxin binding sites and hippocampal fast nicotinic currents. J. Neurosci. 17, 9165–9171.
Papke, R.L., 2014. Merging old and new perspectives on nicotinic acetylcholine receptors. Biochem. Pharmacol. 89 (1), 1–11.
Picciotto, M.R., Caldarone, B.J., Brunzell, D.H., Zachariou, V., Stevens, T.R., King, S.L., 2001. Neuronal nicotinic acetylcholine receptor subunit knockout mice: physiological and behavioral phenotypes and possible clinical implications. Pharmacol. Ther. 92, 89–108.
Resende, R.R., Adhikari, A., 2009. Cholinergic receptor pathways involved in apoptosis, cell proliferation and neuronal differentiation. Cell Commun. Signal. 7, 20–25.
Richter, K., Mathes, V., Fronius, M., Althaus, M., Hecker, A., Krasteva-Christ, G., Padberg, W., Hone, A.J., McIntosh, J.M., Zakrzewicz, A., Grau, V., 2016. Phosphocholine - an agonist of metabotropic but not of ionotropic functions of α9-containing nicotinic acetylcholine receptors. Sci. Rep. 6, 28660. https://doi.org/10.1038/srep28660.
Rottman, J.E., 1994. Mechanisms of intracellular protein transport. Nature 372, 55–63.
Skok, M., Gergalova, G., Lykhmus, O., Kalashnyk, O., Koval, L., Uspenska, K., 2016. Nicotinic acetylcholine receptors in mitochondria: subunit composition, function and signaling. NeuroTransmitter 3, e1290. https://doi.org/10.14800/nt.1290.
Skok, M.V., Voitenko, L.P., Voitenko, S.V., Lykhmus, E.Y., Kalashnik, E.N., Litvin, T., Tzartos, S.J., Skok, V.I., 1999. Study of α subunit composition of nicotinic acetylcholine receptor in the neurons of autonomic ganglia of the rat with subunit-specific anti-α(181-192) peptide antibodies. Neuroscience (4), 1437–1446.
Sottocasa, G.L., Kuylenstierna, B., Ernster, L., Bergstrand, A.J., 1967. An electron-transport system associated with the outer membrane of liver mitochondria. A biochemical and morphological study. Cell Biol. 32, 415–438.
Takamori, S., Holt, M., Stenius, K., Lemke, E.A., Grønborg, M., Riedel, D., Urlaub, H., Schenck, S., Brügger, B., Ringler, P., Müller, S.A., Rammner, B., Gräter, F., Hub, J.S., De Groot, B.L., Mieskes, G., Moriyama, Y., Klingauf, J., Grubmüller, H., Heuser, J., Wieland, F., Jahn, R., 2006. Molecular anatomy of a trafficking organelle. Cell 127 (4), 831–846.
Trikash, I., Gumenyuk, V., Lishko, V., 2010. The fusion of synaptic vesicle membranes studied by lipid mixing: the R18 fluorescence assay validity. Chem. Phys. Lipids 163 (8), 778–786.
Trikash, I.O., Kolchinskaya, L.I., 2006. Fusion of synaptic vesicles and plasma membrane in the presence of synaptosomal soluble proteins. Neurochem. Int. 49, 270–275.
Trikash, I.O., Volynets, G.P., Remenyak, O.V., Gorchev, V.F., 2008. Docking and fusion of synaptic vesicles in cell-free model system of exocytosis. Neurochem. Int. 53 (6–8), 401–407.
Trikash, I., Gumenyuk, V., Chernyschov, V., 2004. The fusion of isolated synaptic vesicles as a model of final step of exocytosis. Neurophysiology 36, 272–280.
Tsudaka, S., Kanno, T., Nishizaki, T., 2015. Levetiracetam enhances a7 ACh receptor responses by indirectly interacting protein kinase A and protein kinase C. Int. J. Biol. Pharmaceut. Res. 6, 558–562.
Turner, T.J., 2004. Nicotine enhancement of dopamine release by a calcium-dependent increase in the size of the readily releasable pool of synaptic vesicles. J. Neurosci. 24 (50), 11328–11336.
Uspenska, K., Lykhmus, O., Gergalova, G., Chernyshov, V., Arias, H.R., Komisarenko, S., Skok, M., 2017. Nicotine facilitates nicotinic acetylcholine receptor targeting to mitochondria but makes them less susceptible to selective ligands. Neurosci. Lett. 656, 43–50.
Vollono, C., Rollo, E., Romozzi, M., Frisullo, G., Servidei, S., Borghetti, A., Calabres, P., 2020. Focal status epilepticus as unique clinical feature of COVID-19: a case report. Seizure 78, 109–112. https://doi.org/10.1016/j.seizure.2020.04.009.
Wonnacott, S., 2014. Nicotinic ACh Receptors. Tocris Cookson Ltd., pp. 29p.
Yao, J., Nowack, A., Kensel-Hammes, P., Gardner, R.G., Bajjalieh, S.M., 2010. Cotrafficking of SV2 and synaptotagmin at the synapse. J. Neurosci. 30 (16), 5569-5578. https://doi.org/10.1523/JNEUROSCI.4781-09.2010.